

# The X-ray spectrum of the atoll source 4U 1608-52

Marek Gierliński<sup>1,2</sup> and Chris Done<sup>1</sup>

<sup>1</sup>Department of Physics, University of Durham, South Road, Durham DH1 3LE, UK

<sup>2</sup>Obserwatorium Astronomiczne Uniwersytetu Jagiellońskiego, 30-244 Kraków, Orla 171, Poland

Submitted to MNRAS

## ABSTRACT

The transient atoll source 4U 1608-52 had been extensively observed by the Rossi X-ray Timing Explorer (*RXTE*) during its 1998 outburst. We analyse its X-ray spectra as a function of inferred accretion rate from both the 1998 outburst and from the non-outburst 1996 and 1998 data. We can fit all the spectra by a model in which seed photons from the neutron star surface are Comptonized in a boundary layer. The Comptonized emission illuminates the accretion disc surface, producing an ionized, relativistically broadened reflection signature, while the direct emission from the accretion disc can also be seen. The evolution of the source can be explained if the main parameter driving the spectral evolution is the average mass accretion rate, which determines the truncation radius of the inner accretion disc. At low mass accretion rates, in the island state, the disc truncates before reaching the neutron star surface and the inner accretion flow/boundary layer is mostly optically thin. The disc emission is at too low a temperature to be observed in the *RXTE* spectra, but some of the seed photons from the neutron star can be seen directly through the mostly optically thin boundary layer. At higher mass accretion rates, in the banana state, the disc moves in and the boundary layer becomes much more optically thick so its temperature drops. The disc can then be seen directly, but the seed photons from the neutron star surface cannot as they are buried beneath the increasingly optically thick boundary layer.

**Key words:** accretion, accretion discs – X-rays: individual: 4U 1608-52 – X-rays: binaries

## 1 INTRODUCTION

Low Mass X-ray Binaries (LMXBs) with a neutron star primary can be observationally divided into two main categories, namely atolls and Z sources (Hasinger & van der Klis 1989). This classification is based on changes in both spectral and timing properties as the source varies, and probably reflects differences in both mass accretion rate,  $\dot{M}$ , and magnetic field,  $B$ . The Z sources have high luminosity (typically more than 50 per cent of the Eddington limit) and magnetic field ( $B > 10^9$  G) while the atolls have lower luminosity (generally less than 10 per cent of Eddington) and low magnetic field ( $B \sim 10^8$  G) (Hasinger & van der Klis 1989).

Both atolls and Z-sources show spectral changes which form a well defined track in a colour-colour diagram. The atolls show hard, power-law spectra at low luminosities (island state), which are startlingly like the low/hard spectra of Galactic black hole binaries (e.g. Barret & Vedrenne 1993; van Paradijs & van der Klis 1994; Barret et al. 2000). At higher luminosities the spectra are typically much softer (banana state; e.g. di Salvo et al. 2000; Piraino, Santangelo & Kaaret 2000). The Z sources always show soft spectra,

but there are subtle spectral changes which show up as a Z-shaped track on a colour-colour diagram. Both types of sources move *along* their tracks on the colour-colour diagram on time-scale of hours to days, except the island state of atolls, where motion can take days or weeks. They do not jump between the track branches. Most of the X-ray spectral and timing parameters depend only on the position of a source in this diagram. This is usually parameterized by the curve length,  $S$ , along the track.

Until recently the atolls were thought to show a characteristic C- (or atoll) shaped track on the colour-colour diagram. However, mapping the full range of colour-colour changes for these LMXBs is difficult because the data available from most of the sources show little variability. There are only a few transient LMXBs with enough observations covering wide range of luminosities, to follow the whole track traced out in the colour-colour diagram. In these transient systems the C-shaped path is only a subset of a larger track. At low luminosities, evolution *within* the island state forms an upper branch, turning the C into a Z (Gierliński & Done 2002; Munoz, Remillard & Chakrabarty 2002).

While the colour-colour diagram is clearly useful as a

way of parameterizing the spectral changes, true spectral fitting gives much more information on the underlying physical changes in the source emission. Here we look at the detailed spectral shape of the transient atoll 4U 1608–52 as a function of its position on the colour-colour diagram, and show for the first time that *all* the spectra can be fit with a model in which a Comptonized boundary layer around the neutron star illuminates the accretion disc, giving rise to a relativistically smeared (and often highly ionized) reflected component and iron line. We show that the spectral changes mapped by the colour-colour diagram are consistent with a picture in which increasing average mass accretion rate increases the optical depth of the boundary layer and decreases the inner radius of the accretion disc.

## 2 THE SOURCE

4U 1608–52 is one of the transient neutron star LMXBs, with outbursts triggered by the disc instability which reoccur on time scales of  $\sim 80$  days to 2 years (Lochner & Roussel-Dupré 1994). However, little is known about the system as the optical counterpart is very faint (Grindlay & Liller 1978; Wachter 1997). The distance is likewise poorly known. The current best estimate of 3.6 kpc is from observations of flux saturated (radius expansion, Eddington limited) type I X-ray bursts (e.g. Nakamura et al. 1989). The inclination is constrained only by the fact that there are no eclipses in the X-ray light curve. The neutron star spin may be indicated by the recently detected burst oscillation in *RXTE* at 620 Hz (Muno et al. 2001).

Hasinger and van der Klis (1989) classified 4U 1608–52 as an atoll source from its spectral and timing properties. Mitsuda et al. (1989) observed with *Tenma* a continuous spectral transition from the banana high-luminosity, soft thermal spectrum to the island state with its low-intensity, hard power-law spectrum. They successfully fit these spectra by a two-component model consisting of the multicolour blackbody from the accretion disc and the Comptonized blackbody from the boundary layer. Higher energy observations with BATSE show that the island state power law is cut-off above  $\sim 100$  keV (Zhang et al. 1996). An iron fluorescence line is detected in the *Tenma* X-ray spectra (Suzuki et al. 1984) with intensity weakly correlated with the source flux (Hirano et al. 1987). *Ginga* observations showed spectra in varying stages between the island and banana states, where the iron line (modelled including the Compton reflected component) increased as the spectrum softened and the source moved towards the banana branch (Yoshida et al. 1993).

The power density spectrum of 4U 1608–52 in the island state resembles that of the black holes in the hard state (Yoshida et al. 1993). It is characterized by a flat top noise ( $P_\nu \propto \nu^s$ , with the slope  $s \sim 0$ ) below and a turn-over above a certain frequency,  $\nu_b \sim 0.2$ –1 Hz. There is also a low-frequency quasi-periodic oscillation (QPO) around 2–9 Hz. *RXTE* has seen a similar spectrum, where the high-frequency noise can be represented by the exponentially cut-off power law (Yu et al. 1997). In the banana state the power spectrum consists of very low-frequency noise below  $\sim 1$  Hz (power law with  $s \sim -1$ ), and an exponentially cut-off power law at higher frequencies (Méndez et al. 1999).

Twin kilohertz QPO's were detected by *RXTE* (van Paradijs et al. 1996; Berger et al. 1996; Méndez et al. 1998a) with varying peak separation (Méndez et al. 1998b). A third kilohertz QPO has also been detected (Jonker, Méndez & van der Klis 2000). The kHz QPOs are only found in a limited range of the colour-colour diagram, near the transition between the island and banana states (Méndez et al. 1999).

## 3 DATA ANALYSIS

We have analyzed *RXTE* observations from the 1998 February–April outburst (archival numbers P30062, P30188, and P30502) and from low-luminosity observations in 1996 December (P10094) and 1998 June, August and September (P30419). All these data belong to the Proportional Counter Array (PCA) gain Epoch 3. A conservative prescription to characterise uncertainties in the instrument response is to add 2 per cent systematics to the data for bright sources (e.g. Cui et al. 1997), irrespective of which detector/layer combination and gain epoch are used. However, inspection of data from the Crab shows that in Epoch 3, when using *only* top layer data from detectors 0 and 1, smaller systematics of 0.5 per cent are more appropriate (Wilson & Done 2001). We have repeated this Crab analysis, and found that even using a single absorbed (fixed at  $N_H = 3.2 \times 10^{21} \text{ cm}^{-2}$ ; Massaro et al. 2000) power law gives a reduced  $\chi^2 = 1.1$  with 0.5 per cent systematic errors. This clearly shows that there are no residuals in the response (e.g. features from the Xenon edge at 4.7 keV, or from the rapid decrease in effective area at low energies) of the top layer of detectors 0 and 1 at this level at this time. This is *not* the case for all layers and all detectors, where the reduced  $\chi^2 = 2.2$  with 0.5 per cent systematic errors and there is a clear feature in the residuals at low energies. Thus we use *only* data from Epoch 3, and from the top layer of detectors 0 and 1, and apply 0.5 per cent systematic errors. However, we have checked that our conclusions are robust even to using 1 per cent systematics, although this gives unrealistically low  $\chi^2$  values.

First, we created PCA light-curves for each energy channel in 128 s time bins. We excluded all the data affected by the type I bursts. This gave us 240 ks of PCA data. The light-curves were used to build a colour-colour diagram, defining a soft colour as a ratio of 4–6.4 to 3–4 keV count rates, and a hard colour as a 9.7–16 over 6.4–9.7 keV ratio. These count rates are corrected for the slow variations in the PCA response (van Straaten et al. 2000; see Gierliński & Done 2002 for technical details applied here). The diagram is shown in Fig. 1.

Next, we extracted the PCA and High Energy X-ray Timing Experiment (HEXTE) spectra corresponding to different positions in the colour-colour diagram. We have assumed that 4U 1608–52 shows a Z-shaped track on the diagram, with inferred accretion rate increasing along the Z: from left to right on the upper branch, through the diagonal to the lower branch (Gierliński & Done 2002; Muno et al. 2002). The diagonal branch is sparsely covered in this data selection. We divided the diagram into eight regions (boxes), as shown in Fig. 1, and averaged the spectra over each box. Neutron star LMXBs are known to vary in luminosity at given colours, creating the so-called parallel lines in colour-intensity diagrams (e.g. van der Klis 2001). Therefore, within

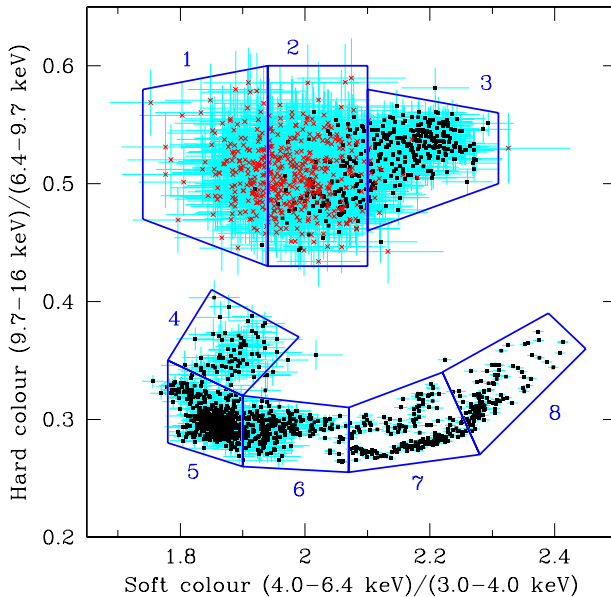


**Figure 1.** Colour-colour diagram of 4U 1608-52. Each point represents 128 s of the data. Slanted crosses correspond to the observations in 1996 December, when the source was at a rather low luminosity, while the squares correspond to the 1998 outburst data. Boxes show selection of the data for spectral analysis. Our choice of the boxes (and their order) follows a Z-shaped track in the colour-colour diagram, which is appropriate for the atolls, as it has been shown recently by Gierliński & Done (2002).

one box we average spectra of different intensities. Though not necessary identical, these spectra should be very similar, considering nearness of colours. In the classic terminology of the atoll sources boxes 1–3 belong to the island state, boxes 5–8 to the banana, while the status of the box 4 cannot be established without joint spectral and timing analysis. To avoid accumulating spectral data from periods distant in time, we have created spectra 1 and 2 from 1996 data only (slanted crosses in Fig. 1), and spectra 3–8 from 1998 data only (filled squares in Fig. 1). The PCA spectra are accompanied by the simultaneous HEXTE spectra extracted from cluster 0. We will refer to these joint spectra as S1–S8.

For spectral fitting we use the X-ray spectral fitting package XSPEC version 11 (Arnaud 1996). The error of each model parameter is given for a 90 per cent confidence interval. We use the 3–20 keV PCA data and 20–150 keV HEXTE data. The relative normalization of the PCA and HEXTE instruments is still uncertain, so we allow this to be an additional free parameter in all spectral fits.

#### 4 SPECTRAL MODEL

Unlike black holes, the accreting neutron stars have both a surface and a magnetic field. Therefore, their X-ray spectra are expected to be more complex than these of the black holes. As well as emission from the accretion flow (direct emission from an optically thick, X-ray illuminated disc and/or an optically thin inner flow, corona or active regions; e.g. Czerny, Czerny & Grindlay 1986; Esin, McClintock & Narayan 1997; Beloborodov 1999) there can be emis-

sion from the neutron star surface and the boundary layer (e.g. Popham & Sunyaev 2001).

Observationally, the X-ray spectra of LMXBs in the soft state are well known to require at least two different spectral components, but the interpretation of these is not unique. The so-called *Eastern* model (Mitsuda et al. 1984, 1989) assumes that the soft component is from the disc, while the hard component is due to Comptonization in the boundary layer or the inner disc. In the *Western* model (White, Stella & Parmar 1988) the soft component is a single-temperature blackbody from the surface, while the hard component is a Comptonized emission from the disc. While it is likely that both disc and boundary layer are Comptonized at some level, it seems more probable that the boundary layer should have a higher temperature than the accretion disc (Popham & Sunyaev 2001).

The hard state X-ray spectra of LMXBs are similar to those of the black hole candidates in their low/hard spectral state. They are dominated by a power law, with some contribution from an additional soft thermal component. The power law is usually interpreted as Comptonization of seed photons in hot, optically thin plasma (see e.g. Barret et al. 2000).

Thus, a physically motivated model which can potentially fit the hard component in *all* spectral states is thermal Comptonization. An optically thin, hot plasma would produce a power-law spectrum (island state), while a plasma with intermediate or high optical depth and lower temperature can create a softer spectrum in which the high energy rollover due to the electron temperature can be seen (banana state). We model the Comptonized spectrum using an approximate solution of Kompaneets (1956) equation (Zdziarski, Johnson & Magdziarz 1996). The model (hereafter THCOMP, not included in the standard distribution of XSPEC) is parameterized by the plasma electron temperature,  $T_e$  and optical depth  $\tau_e$  (or equivalently the asymptotic spectral index), and blackbody seed photon temperature,  $T_{\text{seed}}$ .

The seed photon energy is very important in the Comptonization model, since it gives a low-energy cut-off in the spectrum. For typical mass accretion rates onto a neutron star the seed photons from either the inner accretion disc or neutron star surface should have  $kT_{\text{seed}} \sim 1$  keV. This is plainly not far from the observed X-ray bandpass, so simple analytic approximations (e.g. the COMPST model or a cut-off power law) for the Compton scattered spectrum are *not* valid, since they extend towards lower energies as a uncut power law (see e.g. Done, Życki & Smith 2002). The model THCOMP we use in this paper treats the seed photons low-energy cut-off properly.

The boundary layer should illuminate the inner disc, producing a relativistically broadened iron line and associated reflected continuum. While a broad iron line is often identified in atoll spectra, the reflected continuum which *must* accompany any line emission has only been fit to island state spectra. We calculate the Compton reflection of the THCOMP continuum spectrum using a model where both the continuum reflection and the line are calculated self-consistently for a given ionization state (Życki, Done & Smith 1998). The reflected spectrum (continuum and line) is also relativistically smeared for a given inner disc radius,  $R_{\text{in}}$ . We approximate relativistic smearing by convolving the

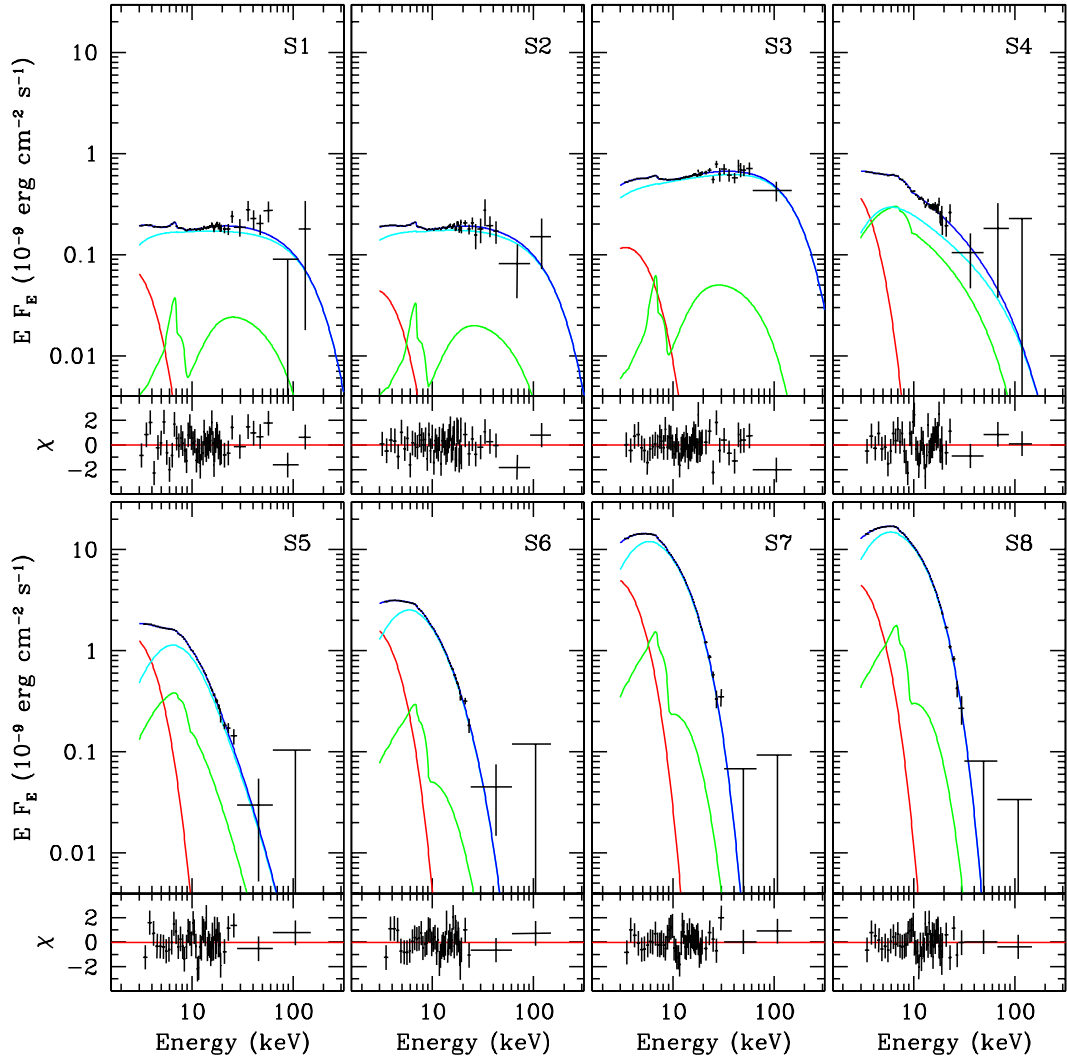


**Figure 2.** PCA/HEXTE spectra of 4U 1608–52 along the atoll track, as selected from the data in Fig. 1. The inferred accretion rate increases from S1 to S8. The individual panels show the unfolded data and models, as well as the residuals. The HEXTE data have been rebinned for clarity. The model, consisting of the disc blackbody (the soft component), Comptonization (the hard component) and its reflection, is described in Section 4. The best-fitting parameters are shown in Fig. 3.

reflected spectrum with a relativistic line profile (Fabian et al. 1989).

First we demonstrate explicitly the need for a two component continuum in *all* the data sets. The THCOMP continuum model and its reflection alone cannot give satisfactory fits for the spectra S1–S5, where  $\chi^2 > 120$  at 80 or 79 degrees of freedom. There is a strong soft excess in the residuals below  $\sim 5$  keV, which is particularly marked in S1 and S5 where  $\chi^2 > 200$ . We use a multicolour disc blackbody (DISKBB in XSPEC; Mitsuda et al. 1984), to describe the soft component. This model is parameterized by the disc temperature,  $T_{\text{soft}}$ , at the inner disc radius ( $R_{\text{in}}$ ) and normalization  $N_{\text{soft}} \propto R_{\text{in}}^2$ . However, its shape is poorly constrained by the RXTE data so it can equally well be a single-temperature blackbody. The spectra S6–S8 give good fits without the soft component ( $\chi^2 = 80, 88$  and  $75$  at  $78$  d.o.f., for S6, S7 and S8, respectively), though even here inclusion of DISKBB improves the fits significantly. The soft component in the case

of the weakest improvement (for S6 where  $\Delta\chi^2 = 11.6$ ) is statistically significant at 99.7 per cent level.

The Compton reflection (including the self-consistent iron line emission) is always significantly detected also. Using the two component continuum model (DISKBB+THCOMP) without a reflected component gives an increase in  $\chi^2$  by more than 50 in all spectra (corresponding to an extremely high significance level).

These results motivate us to choose a model consisting of thermal Comptonization, its Compton reflection and the disc blackbody as the model with which to fit *all* the spectra.

## 5 RESULTS

For spectral fitting we use the model described in the previous section. We apply absorption corresponding to a fixed galactic hydrogen column of  $N_H = 1.5 \times 10^{22} \text{ cm}^{-2}$  (Pen-

**Table 1.** Fitting results of the thermal Comptonization (with Compton reflection) plus disc blackbody model to the spectra S1–S8. The bolometric, unabsorbed flux,  $F_{\text{bol}}$ , was estimated from the model. Units are as follows:  $kT_{\text{seed}}$  and  $kT_{\text{soft}}$  are in keV,  $N_{\text{soft}}^{1/2}$  is in km,  $\xi$  is in  $\text{erg cm s}^{-1}$  and  $F_{\text{bol}}$  is in  $10^{-9} \text{ erg cm}^{-2} \text{ s}^{-1}$ . Brackets in  $kT_e$  column denote the fits in which  $T_e$  was fixed, and its lower limits were calculated additionally (no upper limits were found). Results from this table are visualized in Fig. 3. A detailed description of the model used is in Section 4. The individual spectra are selected from the data as shown in Fig. 1. The spectra and the best-fitting models are shown in Fig. 2.

Obs.	$kT_{\text{seed}}$	$\tau_e$	$kT_e$	$\Omega/2\pi$	$\log(\xi)$	$kT_{\text{soft}}$	$N_{\text{soft}}^{1/2}$	$F_{\text{bol}}$	$\chi^2$
1	$0.51^{+0.70}_{-0.51}$	$1.7^{+0.9}_{-1.7}$	(50) $_{-22}^{+0}$	$0.16^{+0.07}_{-0.06}$	$2.7^{+0.5}_{-0.5}$	$0.68^{+0.08}_{-0.06}$	$7.6^{+2.7}_{-2.5}$	1.0	81.7/78
2	$0.26^{+1.06}_{-0.26}$	$1.7^{+2.9}_{-1.7}$	(50) $_{-38}^{+0}$	$0.17^{+0.09}_{-0.08}$	$2.5^{+1.3}_{-0.7}$	$0.84^{+0.06}_{-0.17}$	$3.5^{+4.3}_{-0.5}$	1.0	70.0/78
3	$0.26^{+0.90}_{-0.26}$	$1.9^{+1.3}_{-1.9}$	(50) $_{-26}^{+0}$	$0.07^{+0.04}_{-0.03}$	$2.8^{+0.8}_{-0.4}$	$1.16^{+0.11}_{-0.16}$	$2.7^{+1.3}_{-0.4}$	3.1	75.0/77
4	$1.01^{+0.23}_{-0.19}$	$1.0^{+1.5}_{-1.0}$	(50) $_{-33}^{+0}$	$0.68^{+1.32}_{-0.48}$	$4.9^{+0.4}_{-0.8}$	$0.63^{+0.13}_{-0.14}$	$22^{+12}_{-8}$	2.4	101.9/77
5	$1.40^{+0.07}_{-0.07}$	$0.4^{+2.3}_{-0.4}$	(50) $_{-45}^{+0}$	$0.23^{+0.12}_{-0.09}$	$4.6^{+0.2}_{-0.3}$	$0.72^{+0.05}_{-0.05}$	$28^{+6}_{-4}$	6.5	106.1/77
6	$1.22^{+0.14}_{-0.11}$	$3.6^{+1.8}_{-2.5}$	$4.9^{+11.5}_{-1.3}$	$0.08^{+0.07}_{-0.02}$	$3.6^{+0.9}_{-0.8}$	$0.75^{+0.10}_{-0.09}$	$28^{+12}_{-6}$	9.7	68.2/76
7	$1.13^{+0.25}_{-0.15}$	$6.0^{+0.8}_{-1.7}$	$3.3^{+0.7}_{-0.2}$	$0.09^{+0.01}_{-0.02}$	$3.4^{+0.6}_{-0.5}$	$0.80^{+0.22}_{-0.11}$	$42^{+43}_{-14}$	36	52.8/76
8	$1.08^{+0.21}_{-0.12}$	$7.2^{+0.7}_{-1.1}$	$3.1^{+0.3}_{-0.1}$	$0.09^{+0.03}_{-0.02}$	$3.5^{+0.7}_{-0.6}$	$0.74^{+0.23}_{-0.20}$	$49^{+60}_{-19}$	42	55.3/76

ninx et al. 1989). In the island state spectra, S1–S3, the HEXTE statistics at higher energies are not good enough to constrain the electron temperature of the Comptonized component,  $T_e$ . The high energy cutoff begins to be seen in S4 and S5, although again the uncertainties on  $T_e$  are large. All of these spectra provide only lower temperature limits. Therefore, we fit the spectra S1–S5 with  $kT_e$  fixed at 50 keV, a value consistent with all these data sets, and then calculate the lower limits on the electron temperature. On the other hand, the spectra S6–S8 are able to constrain the electron temperature well.

The data cannot constrain the inner disc radius from relativistic smearing of the reflected component. Spectral fitting gives only lower limits on  $R_{\text{in}}$ , which are typically  $10\text{--}20R_g$  (where  $R_g \equiv GM/c^2$ ) except for spectra S4 and S5 which are consistent with  $R_{\text{in}} = 6R_g$ . We fix  $R_{\text{in}} = 20R_g$  in all the fits.

We fit all the spectra with the above constraints, and show the spectra unfolded with the best-fitting models in Fig. 2. The best-fitting model parameters are shown in Tab. 1 and Fig. 3.

We calculate the unabsorbed bolometric flux,  $F_{\text{bol}}$ , from the model. We cannot precisely estimate its uncertainties as this depends on the model used as well as on the statistics. However, fits with different soft component model (disc or blackbody) show consistently similar results, with the same trend: an increase from S1 to S3, a drop at S4 and a further increase from S5 to S8. This supports the inferred direction of the increasing accretion rate on the colour-colour diagram, tracing out a Z-shaped track (see also Gierliński & Done 2002).

With increasing inferred accretion rate the spectra become brighter, softer, and have a decreasing electron temperature as seen from the high energy cutoff. The change in the spectral shape between the island and banana states is clearly visible. Spectrum S4 bears more similarities to the banana state spectra than to island state, so it likely belongs to the banana state. The curvature expected from the low energy cut-off in the Comptonized spectrum close to the seed photon energy is clearly seen in spectra S4–S8, where  $kT_{\text{seed}} > 1$  keV. The lower seed photon temperature derived for the island state means the low energy cutoff is less pronounced (not significantly detected) in spectra S1–S3.

The electron temperature of the hard Comptonized component is consistent with a monotonic decline along the colour-colour track, while the optical depth is consistent with a corresponding monotonic increase. These two parameters are difficult to disentangle in data in which the high-energy rollover (at a few  $kT_e$ ) is not observed, as in the island state spectra. However, while the optical depth derived for a given temperature also depends on the assumed geometry, it is clear that the island state spectra have  $\tau_e$  of order unity, while the banana branch has  $\tau_e \gg 1$ . We derive similar optical depths and temperatures when we replace the approximate THCOMP thermal Comptonization model with COMPPS Comptonization code (Poutanen & Svensson 1996), which finds a numerical solution of the Comptonization problem explicitly considering successive scattering orders.

Reflection (mostly driven by the detection of the self consistently produced iron line) is always significantly detected, although the inferred solid angle subtended by the reflecting material is generally rather low, with  $\langle \Omega/2\pi \rangle \approx 0.1$ . The spectrum S4 has somewhat more reflection but this is not strongly statistically significant. Reflection is always strongly ionized, with ionization increasing in the higher luminosity banana spectra. The presence of reflection in all spectra (both in island and banana states) demonstrates that the broad, ionized iron line seen from these sources can indeed be produced by illumination of the accretion disc.

The rather small reflected fraction in the island state is in conflict with  $\Omega/2\pi \approx 0.5\text{--}1$  found in 2–20 keV Ginga X-ray spectra of 4U 1608–52 by Yoshida et al. (1993) and Zdziarski, Lubiński & Smith (1999). This is mostly due to the continuum model used. A power law and its reflected component does indeed give a larger  $\Omega/2\pi$ , but these fits are statistically unacceptable, as well as physically inconsistent. Comptonization *does not* give rise to a power law at energies close to the seed photon energies, and the data also require a soft component as well as the Comptonized emission. Our results are consistent (although with large uncertainties) with a reflection-spectral shape correlation for spectra S1–S4, as claimed by Zdziarski et al. (1999) although there is plainly no *overall* correlation that extends from the island state all the way through the banana branch.

The observed soft component shows rather complex be-

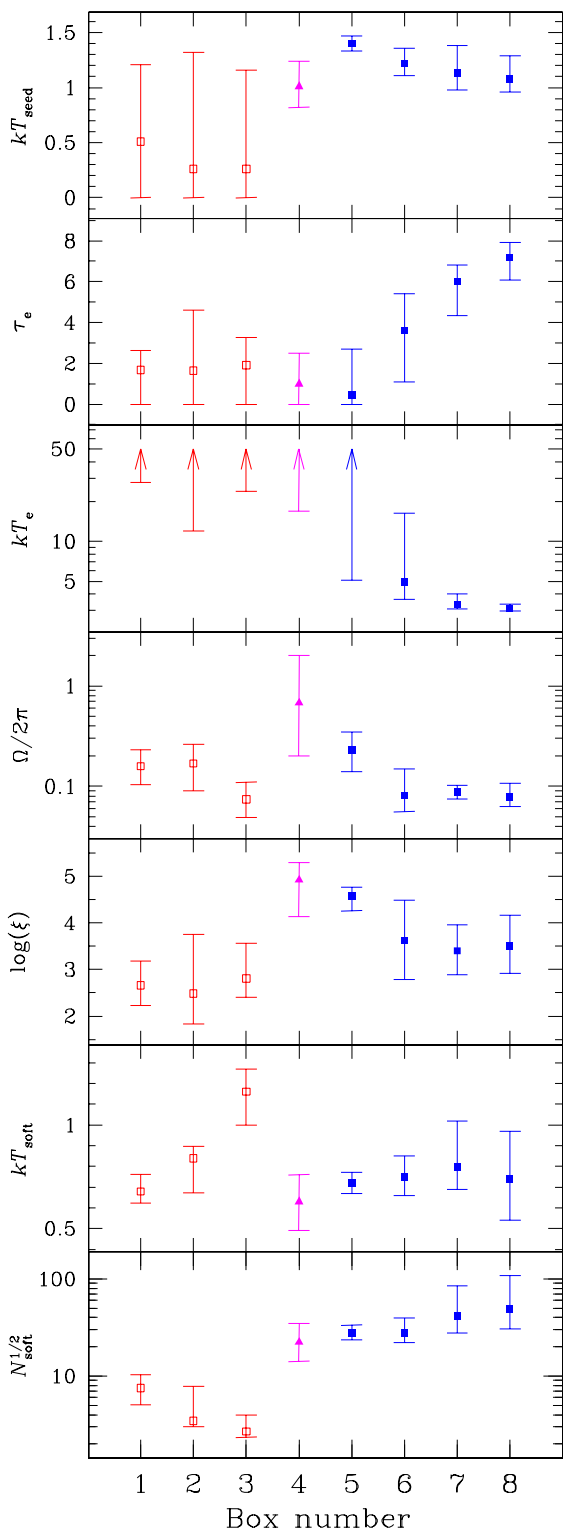


**Figure 3.** Results from Tab. 1. Units are as follows:  $kT_{\text{soft}}$  and  $kT_{\text{seed}}$  are in keV,  $N_{\text{soft}}^{1/2}$  is in km,  $\xi$  is in  $\text{erg cm s}^{-1}$  and  $F_{\text{bol}}$  is in  $10^{-9} \text{ erg cm}^{-2} \text{ s}^{-1}$ . While fitting spectra S1–S5  $T_e$  was fixed at 50 keV, and its lower limits were calculated additionally (no upper limits were found). The symbols used here correspond to the symbols in Figs. 4 and 5. We note that the box number on the horizontal axis does not exactly correspond to the curve length in the colour-colour diagram, and in particular, there is a gap between boxes 3 and 4.

haviour. Fig. 4 shows the soft component flux derived from the model given in Table 1, versus its temperature,  $T_{\text{soft}}$ . There is a striking difference between the behaviour of the soft component in the island and banana states. The figure also shows the curve  $F_{\text{soft}} \propto T_{\text{soft}}^4$ , as expected if the disc geometry remained constant. The uncertainties are large, but while the banana state spectra could be consistent with this relation, the island state is clearly not. This can be also seen from the fitting results (Fig. 3), where the normalization  $N_{\text{soft}} \propto R_{\text{in}}^2$  is fairly constant along the banana track

The difference in the soft component between the island and banana can be further seen in Fig. 5. The seed photons temperature is systematically higher than the soft component temperature in the banana state. Though 90 per cent confidence errors for  $T_{\text{seed}}$  and  $T_{\text{soft}}$  overlap (see Tab. 1), these two parameters are correlated and a fit with forced  $T_{\text{seed}} = T_{\text{soft}}$  is significantly worse. In the island state the uncertainties on these temperatures are substantial but  $T_{\text{seed}}$  is consistent with being equal to  $T_{\text{soft}}$ , and the soft component can be the source of seed photons. This result does not change when we use a single-temperature blackbody instead of the multicolour disc. Conversely, in the banana state, the observed soft component is *not* the source of seed photons for the Comptonized component.

In the island state, the observed seed photons (which are consistent with being the seed photons) have rather low normalization. If these were emitted from a disc then the inner disc radius can be estimated from the DISKBB model as

$$R_{\text{in}} \approx 0.61 N_{\text{soft}}^{1/2} \frac{2.7}{\eta} \frac{D}{3.6 \text{ kpc}} \left( \frac{f_{\text{col}}}{1.8} \right)^2 \left( \frac{0.5}{\cos i} \right)^{1/2} \text{ km}, \quad (1)$$

where  $D$  is the distance to the source,  $i$  is the inclination angle of the disc,  $f_{\text{col}}$  is the ratio of the colour to effective temperature (Shimura & Takahara 1995) and  $\eta$  is the correction factor for the inner torque-free boundary condition (Gierliński et al. 1999:  $\eta = 2.7$  for  $R_{\text{in}} = 6R_g$  and less for higher  $R_{\text{in}}$ ). With  $\eta = 2.7$ ,  $D = 3.6$  kpc,  $f_{\text{col}} = 1.8$  and  $\cos i = 0.5$  we find  $R_{\text{in}} < 5$  km for S1–S3. This is less than the expected neutron star radius of  $\sim 10$  km, and suggests that though we fit the soft component by a disc model, it might not be a disc at all. Even if the colour temperature correction is as high as  $f_{\text{col}} = 2.7$  (Merloni, Fabian & Ross 2000), then S3 still yields  $R_{\text{in}} < 5.5$  km. There are of course more unknowns in Eq. (1), in particular the inclination angle, but  $R_{\text{in}} > 10$  km requires  $i > 81^\circ$ , which is excluded by the lack of X-ray eclipses.

It is therefore unlikely that the soft component is the accretion disc in the island state. Instead, we suggest it comes from the neutron star surface. A fit of a model including a single-temperature blackbody instead of a disc to the island state data yields an apparent radius of the blackbody of  $4 \pm 2$  km.

Conversely, in the banana states, the soft component is consistent with emission from the accretion disc, although these photons do *not* provide the seed photons for Compton scattering. The inner disc radius is consistent with remaining constant throughout the banana state. From the fit to the typical banana spectrum S6 we estimate  $R_{\text{in}} \approx 30$  km, a value consistent with the disc truncated not very far from the neutron star.

If the soft component is the neutron star surface in the

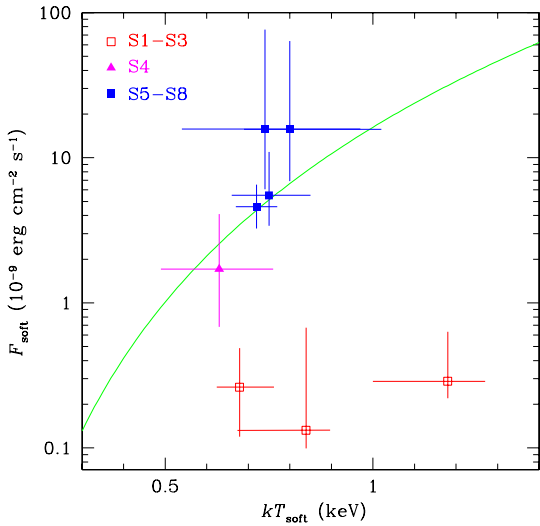


**Figure 4.** Soft component flux versus its temperature. The curve represents the best fit of a function  $F_{\text{soft}} = AT_{\text{soft}}^4$  to the spectra S4–S8. The island state spectra S1–S3 are not consistent with this relation.

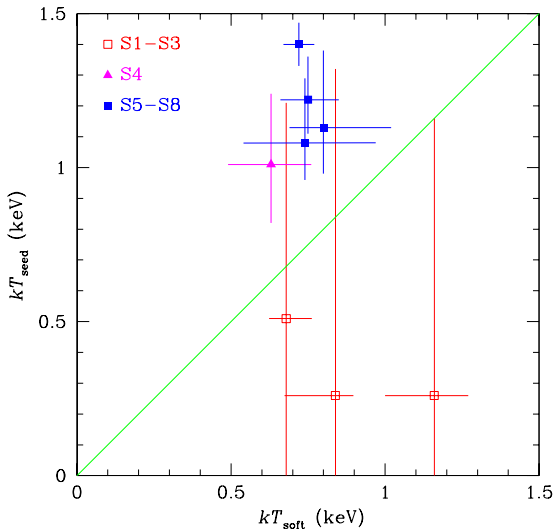


**Figure 5.** Seed photons temperature versus soft component temperature. The line shows where  $T_{\text{seed}} = T_{\text{soft}}$ . In the banana state (S4–S8)  $T_{\text{seed}}$  is systematically higher than  $T_{\text{soft}}$ , therefore the soft component cannot be the source of seed photons. In the island state (S1–S3) the uncertainties are large, but it is possible that the soft component is the source of seed photons.

spectra S1–S3 and the accretion disc in the spectra S4–S8, then the change of trend in  $T_{\text{soft}}$  and  $N_{\text{soft}}$  between S3 and S4 (see Fig. 3) is naturally explained, and does not contradict our assumption about the direction of increase in the accretion rate in the upper branch in the colour–colour diagram. We discuss a physical picture for the evolution of the soft and seed photons in Section 7.

## 6 COMPARISON TO OTHER SOURCES

The X-ray spectra of 4U 1608–52 analyzed here are entirely typical of atoll sources. Having a good coverage of a large luminosity variation, we can compare our results to previous observations of other atolls in various luminosity states.

The island state is characterized by a hard, power-law spectrum, similar to the hard state of black hole binaries, though a bit softer. The presence of a soft component has been reported before in SAX J1808.4–3658 (Gierliński, Done & Barret 2002), 4U 1724–308 (Guainazzi et al. 1998), 1E 1724–3045 and SLX 1735–269 (Barret et al. 2000). In these sources, the radius of the soft component is not consistent with the accretion disc (except perhaps SLX 1735–269, though there is Galactic bulge emission component in the spectrum, which makes spectral modelling difficult; see Barret et al. 2000). This is consistent with what we find in 4U 1608–52 and suggestive that the soft component arises from the neutron star surface rather than from the accretion disc.

The banana state X-ray spectra are soft, and here again the 4U 1608–52 is entirely similar to other atolls. A two-component model has been successfully applied to e.g. KS 1731–260 (Narita, Grindlay & Barret 2001), GX 3+1, Ser X-1 (Oosterbroek et al. 2001) and MXB 1728–34 (di Salvo et al. 2000), the soft component being consistent with the disc. On the other hand, one must be very cautious here, since the soft component properties strongly depend on the Comptonization model applied, and inappropriate approximations have often been used (see Done et al. 2001 for details).

The ambiguity in the spectral shape of the soft component has been reported before (e.g. Guainazzi et al. 1998; Barret et al. 2000). Interestingly, in MXB 1728–34, even *BeppoSAX* spectra which extend down to much lower energies than the PCA cannot distinguish between a disc and blackbody spectrum for the soft component (see di Salvo et al. 2000).

Compton reflection has been reported before in the island state, in e.g. SAX 1808.4–3658 (Gierliński et al. 2002), 4U 1728–34 (Narita et al. 2001), 4U 0614+091 (Piraino et al. 1999), GS 1826–238 and SLX 1735–269 (Barret et al. 2000). However, this paper shows the first detection of reflection in the banana state. Previous work has generally fit an *ad hoc* broad Fe K $\alpha$  line, rather than including the self consistently produced reflected continuum e.g. in GX 3+1, Ser X-1 (Oosterbroek et al. 2001) and 4U 1728–34 (Piraino, Santangelo & Kaaret 2000; Di Salvo et al. 2000).

## 7 DISCUSSION AND CONCLUSIONS

We fit the spectra of the atoll 4U 1608–52 at all points along its track on the colour–colour diagram by a physically motivated model, consisting of thermal Comptonization and its Compton reflection, together with a soft component. Both reflection (with the self consistently calculated iron line emission) and the soft component are always statistically significantly detected in the spectra.

There is a dramatic change in spectral shape between the island and banana states, probably caused by an equally dramatic change in the accretion flow geometry. In the island state the observed soft component luminosity and temperature implies an emission region which is smaller than an

accretion disc around a neutron star. We suggest it arises from optically thick, thermal emission from surface of the neutron star. The hard component is consistent with Comptonization of these observed soft photons from the neutron star surface by hot electrons in an inner optically thin accretion flow (or outer boundary layer). The optically thin Comptonizing medium has temperature of  $\gtrsim 20$  keV. We do not see direct emission from the accretion disc in the PCA energy range, but we do see weak reflected emission implying that the disc subtends a solid angle  $\sim 0.1 \times 2\pi$  from the point of view of the hard X-ray source.

In the banana branch spectra the Comptonized component is much softer, with temperature of  $\sim 5$  keV and optical depth of  $\gg 1$ . Here the observed soft component is consistent with being from the disc, but the seed photons are *not* consistent with being the observed soft component, and again it is more likely that the seed photons are produced predominantly by the neutron star surface. This interpretation favours the Eastern model of LMXBs on the banana branch.

A scenario consistent with all of the above results is one in which the main parameter driving the spectral evolution is the average mass accretion rate, which determines the truncation radius of the inner accretion disc. At low mass accretion rates the optically thick disc does not extend down to the neutron star surface, and the inner accretion flow/boundary layer is mostly optically thin. The large radius of the optically thick disc means that its temperature and luminosity is low so it cannot be seen directly in the PCA spectra, and it subtends a rather small solid angle for reflection. Since the accretion flow is not very optically thick then some fraction  $\sim e^{-\tau} \sim 0.3$  of the emission from the neutron star surface can be seen directly, while the rest is Comptonized into the hard component. As the mass accretion rate increases, so the disc extends further in and the optical depth of the inner flow/boundary layer increases. Eventually the neutron star surface is shrouded by the increasingly optically thick flow, so that these seed photons cannot be seen. The high optical depth also means that the boundary layer emission is then close to thermalizing, so its temperature drops, while the decreasing inner radius of the disc means that its emission starts to become more important in the PCA bandpass.

In this scenario the island state/banana branch transition is marked by the point at which the inner accretion flow collapses into a disc. The disc extends further in so that it is observed more easily as a soft component, softening the soft colour. But it also means that the boundary layer becomes much more optically thick, so its temperature drops, softening the hard colour.

It is plain that this can explain *qualitatively* the atoll source evolution. We will investigate the *quantitative* implications of this in a later paper.

## ACKNOWLEDGEMENTS

This research has been supported in part by the Polish KBN grant 2P03D00514.

## REFERENCES

Arnaud K. A., 1996, in Jacoby G. H., Barnes J., eds., Astronomical Data Analysis Software and Systems V. ASP Conf. Series Vol. 101, San Francisco, p. 17

Barret D., Vedrenne G., 1994, ApJSS, 92, 505

Barret D., Olive J. F., Boirin L., Done C., Skinner G. K., Grindlay J. E., 2000, ApJ, 533, 329

Beloborodov A. M., 1999, ApJ, 510, L123

Berger M., et al., 1996, ApJ, 469, L13

Cui W., Heindl W. A., Rothschild R. E., Zhang S. N., Jahoda K., Focke W., 1997, ApJ, 474, L57

Czerny B., Czerny M., Grindlay J. E., 1986, ApJ, 311, 241

Di Salvo T., Iaria R., Burderi L., Robba N. R., 2000, ApJ, 542, 1034

Done C., Życki P. T., Smith D. A., 2002, MNRAS, 331, 453

Esin A. A., McClintock J. E., Narayan R., 1997, ApJ, 489, 865

Fabian A., Rees M. J., Stella L., White N. E., 1989, MNRAS, 238, 729

Gierliński M., Done C., 2002, MNRAS, 331, L47

Gierliński M., Zdziarski A. A., Poutanen J., Coppi P. S., Ebisawa K., Johnson W. N., 1999, MNRAS, 309, 496

Gierliński M., Done C., Barret D., 2002, MNRAS, 331, 141

Grindlay J. E., Liller W., 1978, L127

Guainazzi M., Parmar A. N., Segreto A., Stella L., dal Fiume D., Oosterbroek T., 1998, A&A, 339, 802

Hasinger G., van der Klis M., 1989, A&A, 225, 79

Hirano T., Hayakawa S., Nagase F., Masai K., Mitsuda K., 1987, PASJ, 39, 619

Jonker P. G., Méndez M., van der Klis M., 2000, ApJ, 540, L29

King A. R., Kolb U., Burderi L., 1996, ApJ, 464, L127

Kompaneets A. S., 1956, Soviet Phys., JETP 31, 876

Lochner J. C., Roussel-Dupré D., ApJ, 435, 840

Massaro E., Cusumano G., Litterio M., Mineo T., 2000, A&A, 361, 695

Méndez M., et al., 1998a, ApJ, 494, L65

Méndez M., van der Klis M., Wijnands R., Ford E. C., van Paradijs J., Vaughan B. A., 1998b, ApJ, 505, L23

Méndez M., van der Klis M., Ford E. C., Wijnands R., van Paradijs J., 1999, ApJ, 511, L49

Merloni A., Fabian A. C., Ross R. R., 2000, MNRAS, 313, 193

Mitsuda K., et al., 1984, PASJ, 36, 741

Mitsuda K., Inoue H., Nakamura N., Tanaka Y., 1989, PASJ, 41, 97

Muno M. P., Chakrabarty D., Galloway D. K., Savov P., 2001, ApJ, 553, L157

Muno M. P., Remillard R. A., Chakrabarty D., 2002, ApJ, 568, L35

Nakamura N., Dotani T., Inoue H., Mitsuda K., Tanaka Y., Matsuoka M., 1989, PASJ, 41, 617

Narita T., Grindlay J. E., Barret D., 2001, ApJ, 547, 420

Oosterbroek T., Barret D., Guainazzi M., Ford E. C., 2001, A&A, 366, 138

Piraino S., Santangelo A., Ford E. C., Kaaret P., 1999, A&A, 349, L77

Piraino S., Santangelo A., Kaaret P., 2000, A&A, 360, L35

Popham R., Sunyaev R., 2001, 547, 355

Poutanen J., Svensson R., 1996, ApJ, 470, 249

Shimura T., Takahara F., 1995, ApJ, 445, 780

Suzuki K., Matsuoka M., Inoue H., Mitsuda K., Tanaka Y., Ohashi T., Hirano T., Miyamoto S., 1984, PASJ, 36, 761

van der Klis M., 2001, ApJ, 561, 943

van Paradijs J., van der Klis M., 1994, A&A, 281, L17

van Paradijs J., et al., 1996, IAUC 6336

van Straaten S., Ford E. C., van der Klis M., Méndez M., Kaaret P., 2000, ApJ, 540, 1049

Wachter S., 1997, ApJ, 485, 839

Wachter S., 1997, ApJ, 485, 839

White N. E., Stella L., Parmar A. N., 1988, ApJ, 324, 363  
Wilson C. D., Done C., 2001, MNRAS, 325, 167  
Yoshida K., Mitsuda K., Ebisawa K., Ueda Y., Fujimoto R.,  
Taqoob T., Done C., 1993, PASJ, 45, 605  
Yu W., et al., 1997, ApJ, 490, L153  
Zdziarski A. A., Johnson W. N., Magdziarz P., 1996, MNRAS,  
283, 193  
Zdziarski A. A., Lubinski P., Smith D. A., 1999, MNRAS, 303,  
L11  
Zhang S. N. et al., 1996, A&AS, 120, 279  
Życki P., Done C., Smith D. A., 1998, ApJ, 496, L25